LBL-13329
Preprint

Lawrence Berkeley Laboratory
UNIVERSITY OF CALIFORNIA

Materials & Molecular Research Division

OCT 26 1981
LIBRARY AND DOCUMENTS SECTION

Submitted to the Journal of Chemical Physics

ELECTRON IMPACT DISSOCIATION OF $CH_4(CD_4)$: LASER INDUCED FLUORESCENCE OF PRODUCT $CH^+(CD^+)$

Bruce H. Mahan and Anthony O'Keefe

September 1981

TWO-WEEK LOAN COPY

This is a Library Circulating Copy which may be borrowed for two weeks. For a personal retention copy, call Tech. Info. Division, Ext. 6782

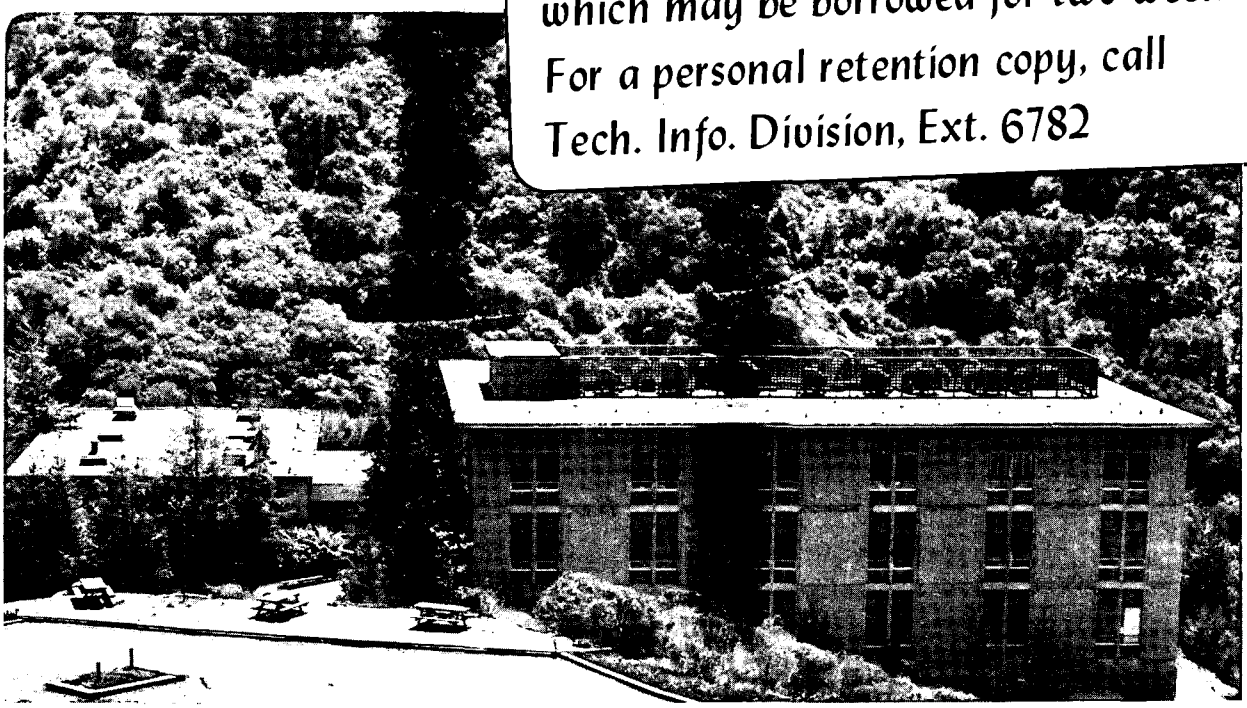

LBL-13329 c.2

Prepared for the U.S. Department of Energy under Contract W-7405-ENG-48

DISCLAIMER

This document was prepared as an account of work sponsored by the United States Government. While this document is believed to contain correct information, neither the United States Government nor any agency thereof, nor the Regents of the University of California, nor any of their employees, makes any warranty, express or implied, or assumes any legal responsibility for the accuracy, completeness, or usefulness of any information, apparatus, product, or process disclosed, or represents that its use would not infringe privately owned rights. Reference herein to any specific commercial product, process, or service by its trade name, trademark, manufacturer, or otherwise, does not necessarily constitute or imply its endorsement, recommendation, or favoring by the United States Government or any agency thereof, or the Regents of the University of California. The views and opinions of authors expressed herein do not necessarily state or reflect those of the United States Government or any agency thereof or the Regents of the University of California.

Electron Impact Dissociation of $CH_4(CD_4)$: Laser Induced Fluorescence of Product $CH^+(CD^+)$

Bruce H. Mahan and Anthony O'Keefe*

Department of Chemistry
and
Lawrence Berkeley Laboratory
University of California
Berkeley, CA 94720

This work was supported by the Director, Office of Energy Research, Office of Basic Energy Sciences, Chemical Sciences Division of the U.S. Department of Energy under Contract Number W-7405-ENG-48.

* Present address: DOC/NOAA/ERL Aeronomy Lab
U. S. Department of Commerce
325 Broadway 1-3522
Boulder, CO 80303

Abstract

Using a 3-dimensional rf quadrupole ion trap to spacially isolate and mass select ions, the laser induced fluorescence spectra of the CH^+ and CD^+ $A^1\Pi$ - $X^1\Sigma^+$ system has been recorded. The fragment ions were produced by the electron impact ionization of CH_4 and CD_4. Many new ro-vibronic components of this system were observed permitting a refinement of existing molecular constants. The observation of transitions involving CD^+ $^1\Sigma^+$ v=2 provides the first experimental determination of the $X^1\Sigma^+$ state vibrational frequency.

The distribution of energy among the product $CH^+(CD^+)$ vibrational and rotational modes has been determined. Since the ions are studied under collision free conditions the observed distribution can be used to study the dissociation pathways leading to the production of $CH^+(CD^+)$.

The mechanisms leading to the unimolecular dissociation of polyatomic molecules have been the focus of many experimental and theoretical investigations in the past. The ideal experimental study of such processes involves, first, the preparation of the reagent molecule in a specific quantum state, specifying the degree of rotational, vibrational and electronic excitation. Following the dissociation, the distribution of the available reaction exothermicity among the products is measured in some fashion. The development of powerful tunable lasers has resulted in initial quantum state selection as well as product state determination via laser induced fluorescence in favorable situations.[1-2] Product energy distribution analysis at lower energy resolution is afforded by the molecular beam time of flight technique which permits the resolution of some vibrational and most electronic product distributions.

While the techniques listed above have provided important information on the unimolecular processes involving neutral species they have not yet proven to be useful in the study of molecular ions. While small organic cations are known to play crucial roles in both combustion and interstellar chemistry, the role played by the excited vibrational and electronic states of such ions is not well understood. Studies of excited molecular ions and ion molecule reactions have been limited to the

measurement of appearance potentials which offers little insight into the actual distribution of reaction exothermicity. The major obstacles to the study of molecular ions are the low densities in which ions are typically formed and the great reactivity of molecular ions in general.

Using a quadrupole ion trap of cylindrical design we have studied several molecular ions using laser induced fluorescence.[3-7] The use of an ion trap permits the selection and storage of specific ions under collision free conditions. Alternatively, collisions may be allowed under controlled conditions and the effects of such collisions upon the stored ions studied. In this fashion we have recently measured a strong dependence of the charge transfer cross section for the reaction.

$$N_2^+(X^2\Sigma^+_{gv=0,1}) + Ar \rightarrow N_2(X^1\Sigma^+_{gv=0}) + Ar^+ .$$ [7]

In the present study the internal energy distribution of $CH^+(CD^+)$ produced through electron impact ionization of $CH_4(CD_4)$ is measured. While the initial dissociating state of CH_4^+ is not selected in this study, it will be argued that production of CH^+ probably follows excitation of the $(2a_1)^{-1}$ band of CH_4^+. The observed rotational distributions of several vibrational levels in both the CH^+ and CD^+ ground electronic state $(X^1\Sigma^+)$ are found to be identical, corresponding to a rotational temperature of ~1500°K. In contrast, the observed vibrational distribution is found to be non Boltzmann.

EXPERIMENT

The experimental arrangement used in the present study has been described in detail elsewhere.[3-7] Briefly, the approach involves the use of a three dimensional rf quadrupole ion trap within which ions of a specific charge to mass ratio can be stored. Ion densities of from 10^6 - 10^8 ions/cc can be maintained for time periods of many msec. The ions are formed by a 1 msec pulse of ~100 eV electrons which are directed through the center of the ion trap. The electrons ionize background gas which is introduced to the vacuum chamber housing the ion trap through a variable leak valve and maintained at $\sim 10^{-5}$ Torr. Following ion formation a 10 nsec pulse from a tunable dye laser is passed through the ion cloud and any resulting fluorescence monitored at right angles to the laser beam. The experimental arrangement is schematically depicted in Figure 1. The resulting laser induced fluorescence signal is normalized for variation in laser power as well as variations in the ion density. Since the ions are examined under collision free conditions the distribution of internal energy which characterizes the ion formation processes remains unperturbed with the exception of short lived electronic states. The ion trap is cleared of ions following the fluorescence detection gate period by applying a high voltage pulse to the lower cap electrode and new ions are formed for the following experimental cycle. This process insures the ion population studied in each cycle has a similar history and have not had time to undergo collisions with the background neutral gas molecules. Such

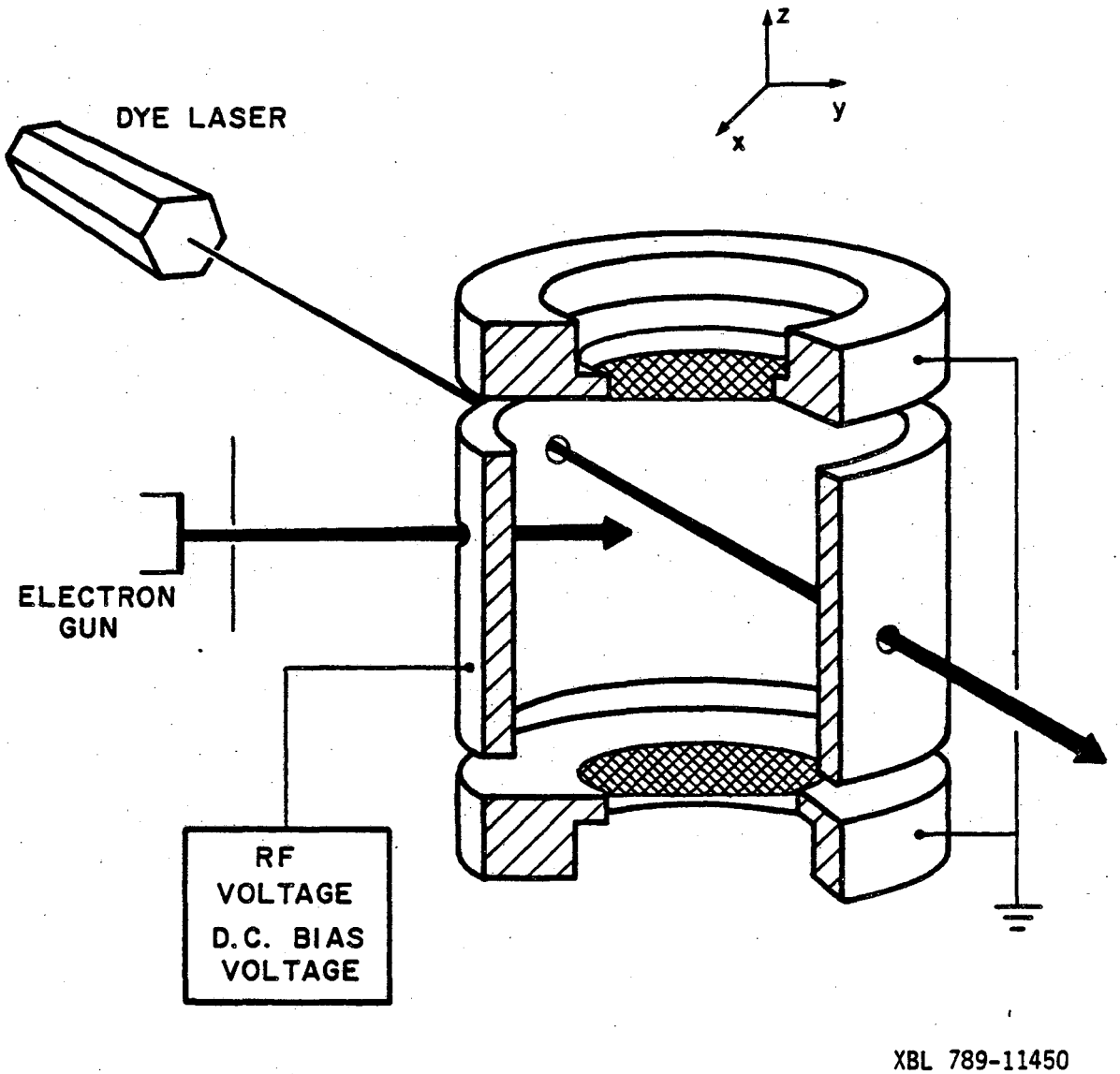
z
y
x
DYE LASER
ELECTRON
GUN
RF
VOLTAGE
D.C. BIAS
VOLTAGE
XBL 789-11450

Figure 1

collisions have already been shown to dramatically alter the rotational and vibrational population distributions of trapped ions.[7] After accumulating fluorescence signal using sensitive photon counting techniques for typically several hundred laser shots the laser wavelength is stepped by 0.1 Å which is smaller than the expected ~0.2 Å doppler width of ions stored in a trap such as ours.[8] The data are stored on floppy disk for later retrieval and analysis.

RESULTS

A. Spectroscopic Results

Laser induced fluorescence spectra were obtained for the (0,0) and (2,1) bands of CH^+ and for the (0,0), (2,1), and (1,2) bands of CD^+. Representative portions of the spectra obtained are presented in Figures 2-4. The rather broad distribution of rotational population, as reflected in the intensity of high J levels, provides a probe of the reaction exothermicity since the ions are maintained in a collision free environment. While portions of the (0,0) and (2,1) bands have been previously observed for both CH^+ and CD^+,[9,10] no transitions involving $V'' \geqslant 2$ have been reported. While only a few members of the R branch in the region of the (1,2) band-head were observed in the present study, spectroscopic constants for the $X^1\Sigma^+$ (v=2) state may be obtained because the upper state ($A^1\Pi$(v=1)) is already well characterized.

Initial estimates of $B''_{v=2}$ and $D''_{v=2}$ can be obtained from existing constants. The values are then varied until the calculated differences in line frequencies most closely match

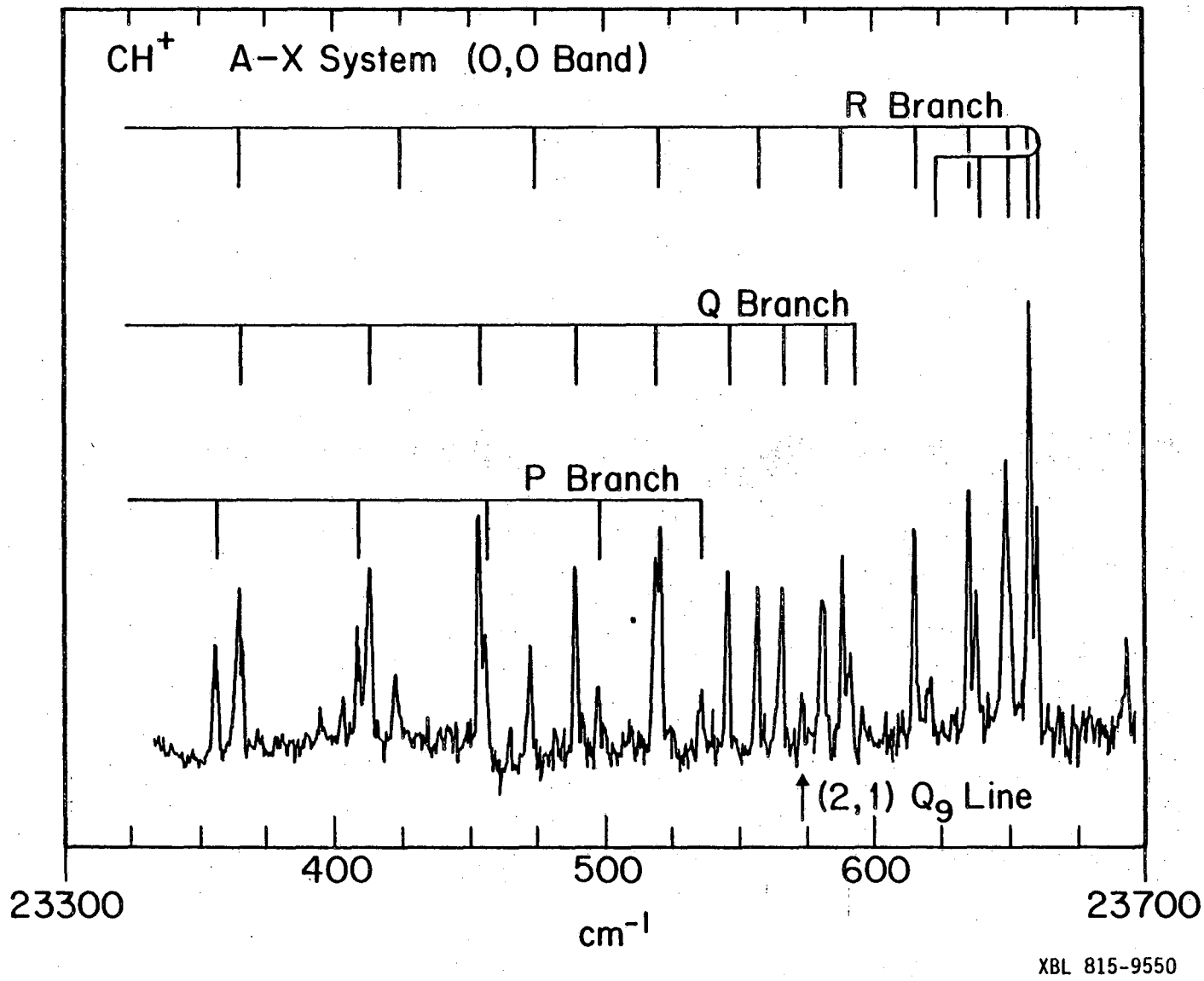
CH+ A–X System (0,0 Band)
R Branch
Q Branch
P Branch
(2,1) Q9 Line
400
500
600
23300
23700
cm-1
XBL 815-9550

Figure 2

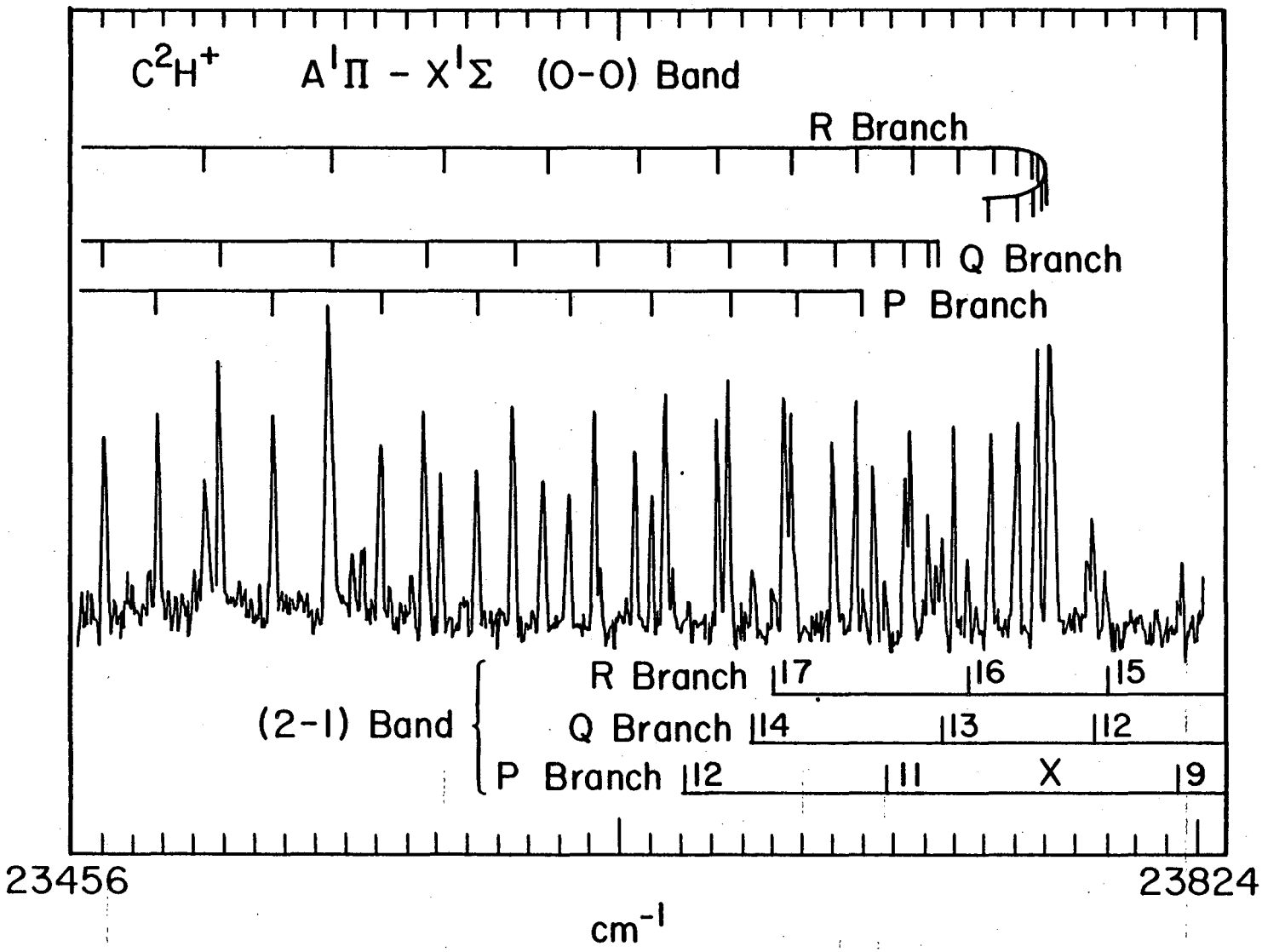

XBL 808-11413

Figure 3

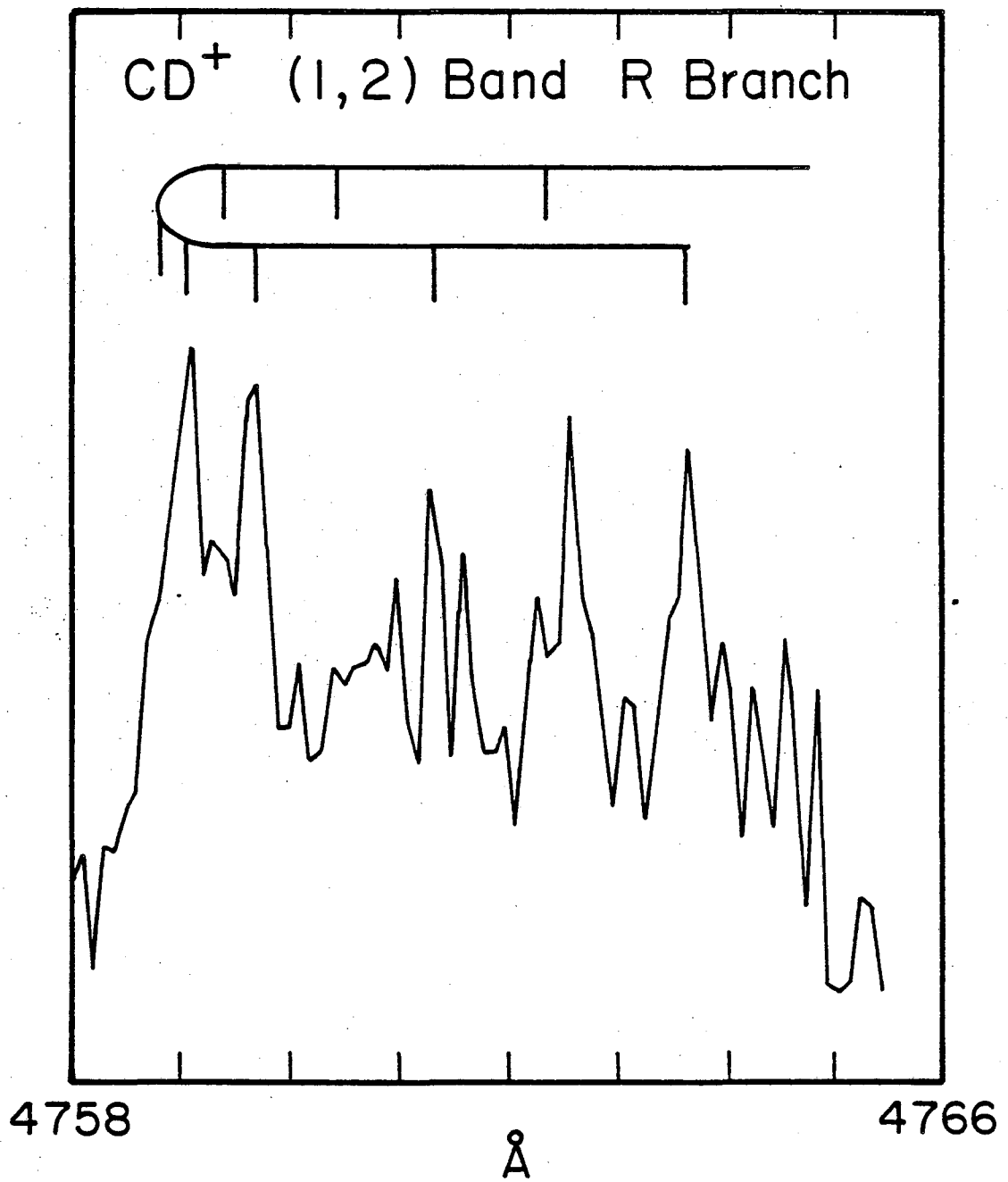

XBL 815-9549

Figure 4

the observed differences. Once the rotational constants have been determined in this fashion, the separation between the band origin and the band head can easily be calculated through the relation[11]

$$\Delta r = \frac{-(B'+B'')^2}{4(B' - B'')} . \qquad (1)$$

The band head of the (1,2) band as determined in this study occurs at 21014.1 cm^{-1}.

Such an analysis results in a rotational constant of B" = 7.22 cm^{-1}, and a resulting band origin of r = 20983.0 cm^{-1}. Observed line frequencies for this band are tabulated in Table I. The agreement between observed and calculated line frequencies is not as good for this band as for the other observed bands of either CD^+ or CH^+. This is due largely to the low signal level and subsequent poor signal to noise ratio of the (1,2) band.

The vibrational frequency we measure for the $X^1\Sigma^+$ state of CD^+ is 2092 cm^{-1} and the corresponding frequency of CH^+, calculated using isotope relations, is 2850 cm^{-1}. Since there have been no published experimental observations of CH^+ or CD^+ in $v'' \geqslant 2$ the frequencies reported here may only be compared with calculated frequencies.[12] The calculations of Green et al.,[13] Banyard and Taylor,[14] and Rosmus and Meyer[15] provide frequencies for CH^+ of 2834 cm^{-1}, 2843 cm^{-1} and 2851 cm^{-1} respectively. The excellent agreement between the experimental results and the calculations of Rosmus and Meyer[15] provide additional verification of the usefulness of the coupled electron pair approach (CEPA) method in the calculation of accurate molecular constants.

Table I. Observed line frequencies (in cm^{-1}) for the CD^+ $A^1\Pi \leftarrow X^1\Sigma^+(1,2)$ band

J	R branch
0	20991.7
1	20998.3
2	21009.3
3	21012.8
4	21014.1
5	21011.5
6	21005.3
7	20996.9

Previous optical emission studies of CH^+ and CD^+ have resulted in the observation of only the lowest few J levels of each observed band. This is due in part to the strong optical interference by other molecular species in the excitation region, and to collisional relaxation of high rotational levels. Since both of these complications are avoided in the present study many previously unobserved rovibronic components of each band studied here have been observed. These high rotational levels provide a sensitive probe of the rotational molecular constants. While the large Doppler width of the trapped ions results in a spectral resolution of ~1 cm^{-1}, the large number of lines observed increases the accuracy with which the molecular constants may be determined. High resolution emission studies of CH^+[9] and CD^+[10] have observed up to J" = 7 for the CH^+(0,0) band and up to J"=11 for the corresponding band in CD^+. The chemiluminescence studies of Ottinger[16] on the $A^1\Pi \rightarrow X^1\Sigma^+$ system of both CH^+ and CD^+ seem to have extended the list of observed but poor spectral resolution (~ 35 cm^{-1}) prevented the refinement of existing molecular constants. The present study has extended the list of observed rotational components out to J = 22 and J = 24 for the (0,0) bands of CH^+ and CD^+ respectively. The observed frequencies of the (0,0) and (2,1) bands have been reported[5] as well as direct measurements of the $A^1\Pi_{v=0}$ radiative lifetime for both CH^+ and CD^+.[3] The molecular constants derived from this data as well that obtained from the previously unobserved (1,2) band of CD^+ are summarized in Tables II and III. These molecular

Table II. Molecular constants (in cm^{-1}) for the CH^+ (0,0) band and calculated vibrational frequency for the $X^1\Sigma^+$ state

V_{00}	23596.88(1)
B^{RP}	11.4546(20)
D^{RP}	.00207(5)
H^{RP}	$3.31(10) \times 10^{-8}$
B^{Q}	11.4148(20)
D^{Q}	.00205(5)
H^{Q}	$3.15(10) \times 10^{-8}$
B"	13.9344(20)
D"	.00141(5)
H"	$6.77(10) \times 10^{-8}$
ω_e	2850.1
$\omega_e\chi_e$	52.9

* Numbers in parentheses represent a one standard deviation uncertainty in the last digits of each constant.

Table III. Molecular constants for the (0,0), (2,1) and (1,2) bands of CD^+. Values in cm^{-1} and Å units

r	23747.54(2)*	24094.87(5)	20983.0(5)
B^{RP}	6.2520(5)	5.4911(7)	5.855
D^{RP}	$5.818(10) \times 10^{-4}$	$8.667(10) \times 10^{-4}$	5.7×10^{-4}
H^{RP}	$2.77(25) \times 10^{-7}$	$2.40(20) \times 10^{-6}$	-
B^{Q}	6.2392(5)	5.4805(5)	5.840
D^{Q}	$5.818(10) \times 10^{-4}$	$6.48(10) \times 10^{-4}$	5.7×10^{-4}
H^{Q}	$2.95(25) \times 10^{-7}$	$8.60(30) \times 10^{-7}$	-
B_e'		6.447(5)	
α_e'		0.39(2)	
R_e'		1.241(3)	
B''	7.5828(5)	7.4015(7)	7.22(1)
D''	$5.819(10) \times 10^{-4}$	$1.126(10) \times 10^{-4}$	.0012(4)
H''	$3.81(10) \times 10^{-7}$	$4.28(5) \times 10^{-6}$	
B_e''		7.763(7)	
α_e''		0.18(2)	
R_e''		1.116(3)	
ω_e		2092	
$\omega_e\chi_e$		28.5	

* See footnote, Table II.

constants were obtained using a weighted least squares fit of all observed members of each band. The relative weighting of new lines observed in the present study to those seen under higher resolution in the emission studies was adjusted empirically until the calculated line frequencies agreed with experimentally determined values to within the reported error limits. These error limits are approximately .05 cm^{-1} for the low J components observed in emission spectra and ~.5 cm^{-1} for new lines observed in this study.

The observed low intensity of the (1,2) band of CD^+ is due primarily to the low populations of excited vibrational levels of the ion. The corresponding band in CH^+ is expected to be much weaker due to the large increase in vibrational energy. While we have not observed this band it is possible to predict its molecular constants using isotope relations. Values arrived at in this fashion are listed in Table II.

In addition to the $A^1\Pi$ - $X^1\Sigma^+$ system, the $^3\Sigma^-$ - $^3\Pi$ system might also extend into the spectral region investigated here (3900 Å - 5000 Å). The triplet system has been seen in emission studies[17] but does not appear to possess appreciable intensity above 3800 Å. No transitions other than those belonging to the $A^1\Pi$ - $X^1\Sigma^+$ system were observed in the present study.

B. Product Energy Distributions

Since the ions are stored under collision free conditions, the rotational and vibrational population distributions, as deduced from the laser induced fluorescence intensities, reflect the dynamical partitioning of reaction exothermicity. If the distribution of energy among all dissociation products

were measured, a detailed analysis of the dissociation dynamics would be possible. In the present study, however, only one fragment of the methane dissociation has been probed. The combination of these results and results obtained in mass spectrometric studies can provide some insight into the dissociation process.

The spectra obtained in Figures 2 and 3 are normalized to variations in laser power with frequency and so the relative line intensities may be used to calculate a rotational temperature. It is possible, however, that the formation of CH^+ occurs via more than one dissociation path and the observed intensity distribution actually the superposition of several distributions. The relative absorption intensities of rotational components within a vibronic band can be approximated by the expression

$$I \simeq K_{abs}\ S_J \exp\left[\frac{-B''J''(J''+1)hc}{kT}\right] \tag{2}$$

where K_{abs} is a constant for a given vibronic band, assuming constant R-centroid, and S_J is the appropriate Hönl-London line strength coefficient for each rovibronic component. Since we are exciting CH^+ from a $^1\Sigma$ state to a $^1\Pi$ state, $\Delta\Lambda = +1$. The Hönl-London factors for the R, P and Q branches which are appropriate for this case are[11]

$$S_J^R = \frac{(J''+2+\Lambda'')(J''+1+\Lambda'')}{4(J''+1)} \tag{3a}$$

$$S_J^P = \frac{(J''-1-\Lambda'')(J''-\Lambda'')}{4J''} \tag{3b}$$

$$S_J^Q = \frac{(J''+1+\Lambda'')(J''-\Lambda'')(2J''+1)}{4J''(J''+1)} \tag{3c}$$

A plot of $\ln (I/S_J)$ vs $J''(J''=1)$ yields a straight line with a slope of $-B''hc/kT$ if the distribution of rotational population can be characterized by an equilibrium temperature.

It is reasonable to expect the dissociation exothermicity of CH_4 in the production of CH^+ to be essentially the same as that of CD_4 producing CD^+. It is of interest to compare the distribution of rotational and vibrational energy in both CH^+ and CD^+. The rotational temperatures of both $CH^+_{(v''=0)}$ and $CD^+_{(v''=0)}$ have been determined by an analysis of the plots shown in Figures 5 and 6 respectively. As can be seen in the plots, the observed rotational distributions are essentially single temperature distributions corresponding to a rotational temperature of ~1500°K. The rotational distributions in higher vibrational levels of the fragment ions are more difficult to ascertain due to the lower intensities of these bands. The (2,1) band of CD^+ is of sufficient intensity due to its smaller vibrational spacing to permit an analysis of its rotational temperature. The result, shown in Fig. 6, is identical to that obtained for the (0,0) band of CD^+, although the absolute intensities are lower due to differences in Franck Condon factors.

The observed intensities of transitions belonging to the CH^+(2,1) band are too low to determine a reliable rotational temperature, however, the strongest members of this band originate in $J'' = 6-8$. This observation is consistent with a rotational temperature identical to that of the (0,0) band.

These results are rather different from those obtained by Cody et al.[1] for the internal energy distributions of the CN radical produced through the photolysis of C_2N_2. In that study

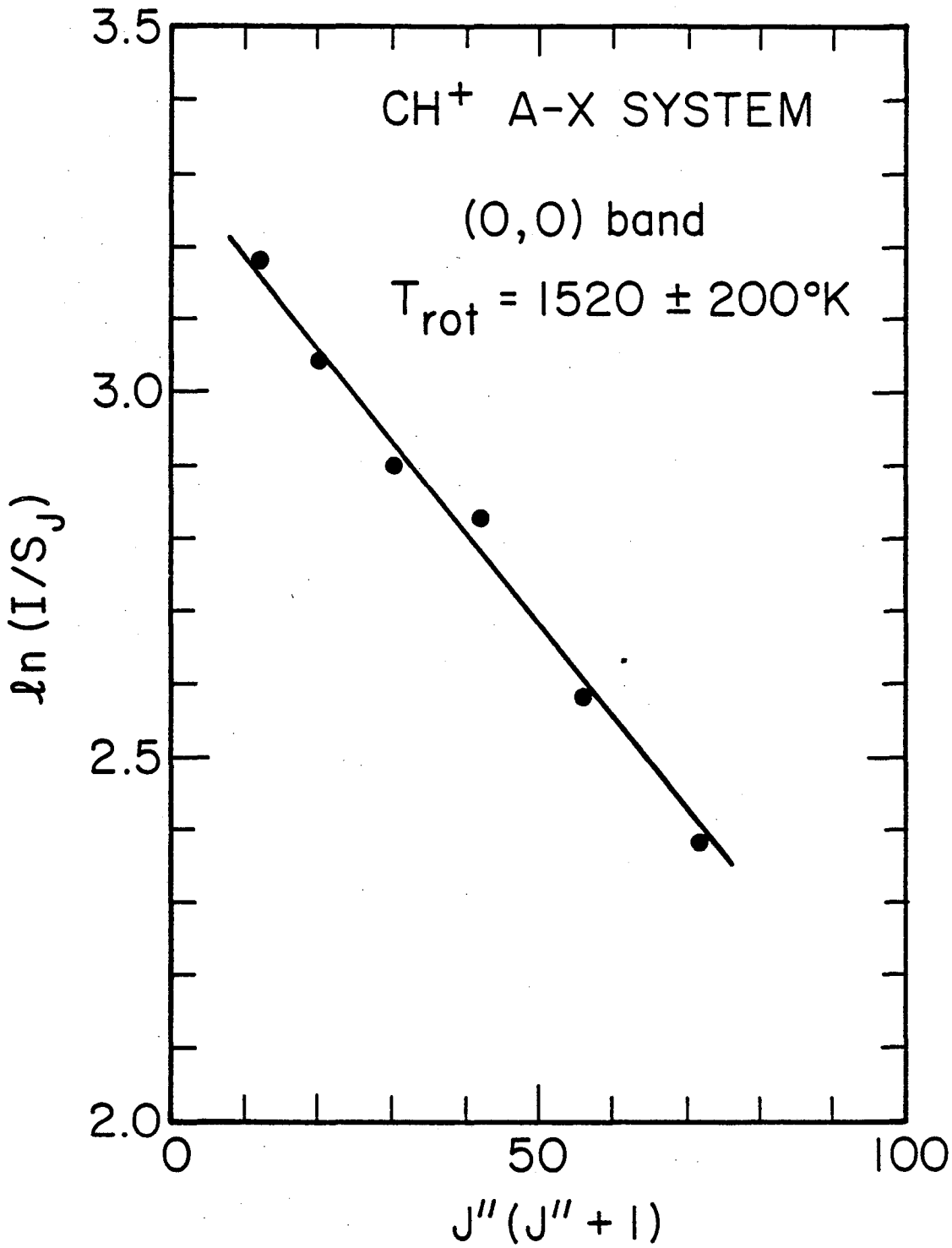

XBL 818-11091

Figure 5

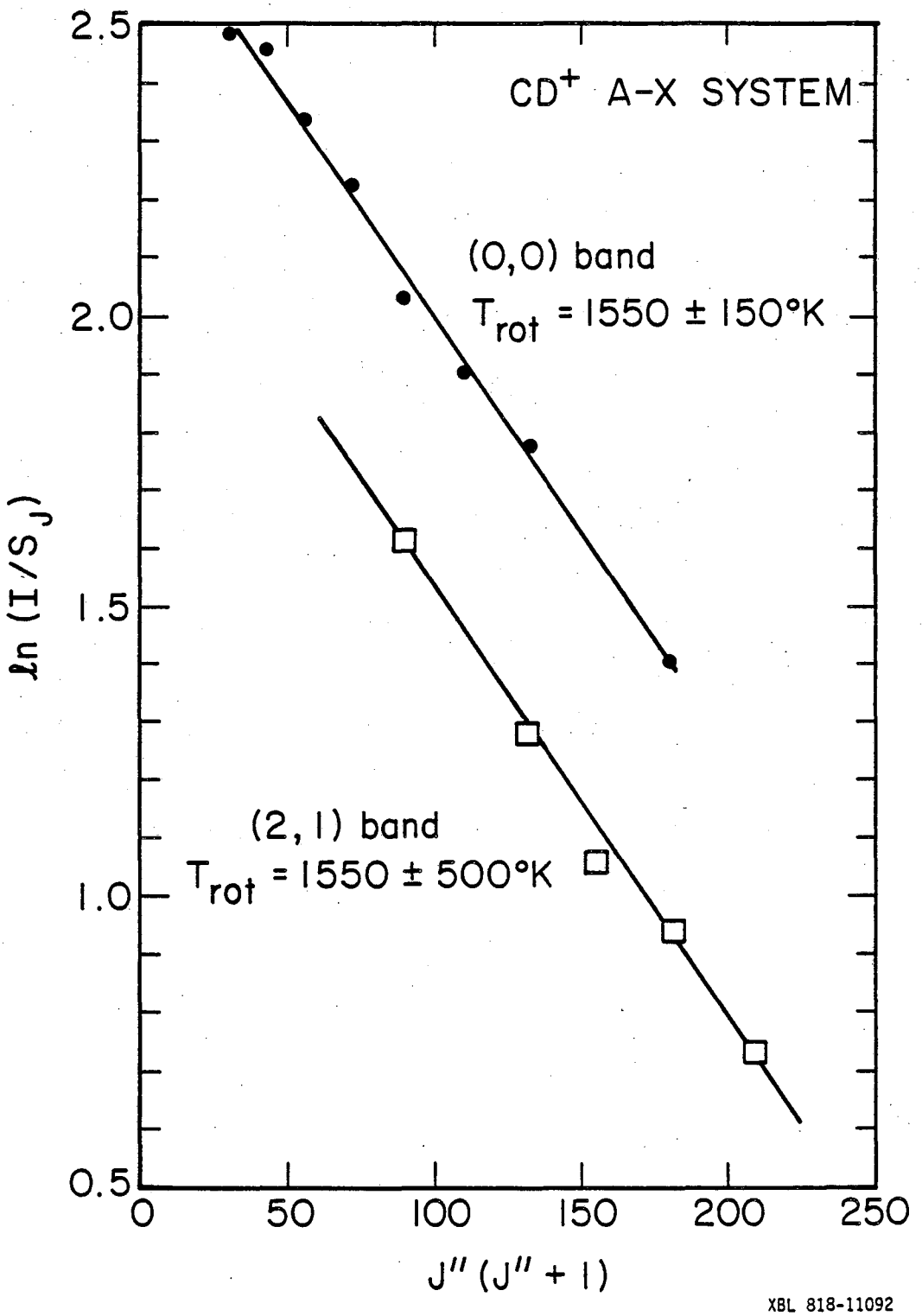
CD+ A-X SYSTEM
(0,0) band
Trot = 1550 ± 150°K
(2,1) band
Trot = 1550 ± 500°K
ln (I/SJ)
J'' (J'' + 1)
2.5
2.0
1.5
1.0
0.5
0
50
100
150
200
250
XBL 818-11092

Figure 6

it was found that the rotational temperature of the radical product decreased slightly with increasing vibrational excitation, reflecting the partitioning of the finite dissociation exothermicity.

In addition to the measurement of rotational energy distributions of CH^+ and CD^+, vibrational populations can be ascertained if the Franck-Condon factors for the relevant vibronic bands are known or can be estimated. Components of both the (0,0) and the (2,1) bands of both CH^+ and CD^+ are easily discerned in Figs 2 and 3. Franck-Condon factors for many bands in the A-X system have been calculated by several authors.[13,16,18] Using those calculated by Gerard et al.,[18] the relative transition strength of the (0,0) to the (2,1) bands should be 2.6 and 2.2 for CH^+ and CD^+ respectively. Since the rotational population distributions of the v'=0 and v''=1 levels of CD^+ have already been shown to be the same we may estimate the vibrational population distribution by weighting the observed transition intensities of corresponding ro-vibronic components by their calculated transition strengths. Several members of the R and Q branches of both bands were used to make the comparison since these bands are the strongest in a $^1\Pi$ - $^1\Sigma$ transition (see eq. 3). The result, for CD^+, is a population ratio of the v' = 0 level to the v'' = 1 level of ~1.1. The vibrational frequency of the CD^+ $X^1\Sigma^+$ state, as determined in the present study is 2092 cm^{-1}, which indicates a vibrational temperature of ~3 x 10^4 °K. If the rotational population distribution of CH^+ $X^1\Sigma^+$(v''=1) is the same as that of the v''=0 level then the vibrational temperature, based upon Franck-Condon

factors and observed intensity ratios, is the same as that of CD^+ within estimated uncertainties in the intensity measurements.

If the distribution of vibrational energy were truely equilibrated to a temperature of 3×10^4 °K then the intensity of the CD^+ (1,2) band, based upon the Franck-Condon factors of Gerard et al.,[18] should be approximately 40% of that seen for the (0,0) band. Careful measurements made in search of the (1,2) band of CD^+ resulted in the observation of the band presented in this paper, but only after extensive signal averaging. While the calculated Franck-Condon factors involving $v'' \geqslant 2$ have not been verified experimentally, the observed intensity variation would require the (1,2) Franck-Condon factor to decrease by roughly an order of magnitude. Thus, it would appear to be more plausible to attribute the intensity variation to real population differences. This would indicate that the vibrational distribution of product $CH^+(CD^+)$ produced in the dissociation of $CH_4(CD_4)$ is non Boltzmann. The relation between the product vibrational state population and the active dissociation mechanisms of CH_4 will be examined later.

C. Discussion

In order to understand the fragmentation processes which lead to the production of CH^+ it is useful to examine the photoelectron data available on methane. Numerous studies have been performed which have provided molecular orbital energies for CH_4^+[19,20] as well as mass spectrometric branching ratios of parent and fragment ions.[21-24] The photoelectron bands observed experimentally are indicated in Fig. 7a, along with their

assignments. The ion is initially formed in the $(1a_1)^2$ $(2a_1)^2$ $(1f_2)^5$ configuration with an appearance potential of ~12.7 eV. The large width of this band is due to the combination of a large change in equilibrium geometry and the Jahn-Teller induced distortion of the ion.[25] At approximately 10 eV higher energy a second band, corresponding to the configuration $(1a_1)^2$ $(2a_1)^1$ $(1f_2)^6$, is seen with an onset at 22.3 eV. In the remaining discussion these states will be referred to as $(1f_2)^{-1}$ and $(2a_1)^{-1}$ respectively (as in Fig. 7). The equilibrium geometries of these two states, as calculated by Meyer,[26] show both to be of tetrahedral structure with a C-H bond length of 2.15 Å for the $(1f_2)^{-1}$ state. This bond distance is to be compared with the 1.09 Å C-H bond length of ground state neutral CH_4. This increase in bond length reflects the removal of a bonding electron in the formation of the ion. The removal of an electron from the $(2a_1)$ orbital results in an increase in the C-H bond length to 2.23 Å. Such a large change in the equilibrium bond length accompaning ionization will surely result in a large degree of vibrational excitation in the newly formed ion. The consequences of this vibrational excitation are seen in Fig. 7b, in which the product branching ratio is plotted as a function of ionization energy. As soon as the formation of CH_3^+ becomes energetically allowed, at about 14 eV,[24] the branching ratio of CH_4^+ to CH_3^+ drops to ~1; a value that remains nearly unchanged for most of the $(1f_2)^{-1}$ band profile.

At the high energy limit of the $(1f_2)^{-1}$ band the formation of CH_2^+ becomes energetically allowed,[24] however, the branching ratio of CH_4^+ to CH_3^+ changes only slightly due to the poor

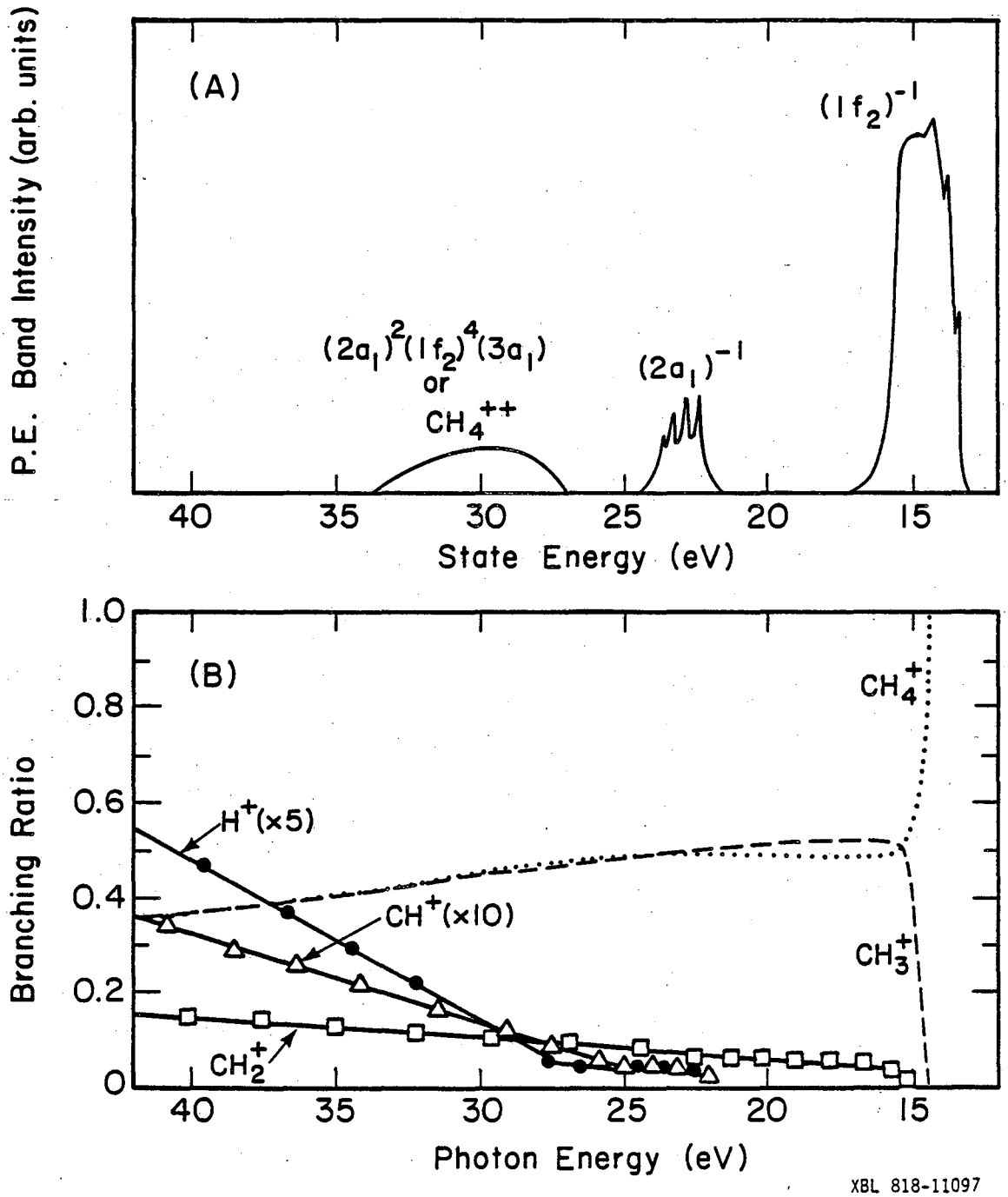
(A)
P.E. Band Intensity (arb. units)
$(1f_2)^{-1}$
$(2a_1)^2(1f_2)^4(3a_1)$
or
CH_4^{++}
$(2a_1)^{-1}$
40
35
30
25
20
15
State Energy (eV)
(B)
Branching Ratio
1.0
0.8
0.6
0.4
0.2
0
CH_4^+
$H^+(\times 5)$
$CH^+(\times 10)$
CH_3^+
CH_2^+
40
35
30
25
20
15
Photon Energy (eV)
XBL 818-11097

Figure 7

geometrical overlap of ground state CH_4 with the highly vibrationally excited levels in $CH_4^+(1f_2)^{-1}$ which decay to produce CH_2^+. The branching ratio does not change significantly until the $(2a_1)^{-1}$ is reached. The onset of the $(2a_1)^{-1}$ band coincides with the appearance potential of the CH^+ fragment as well as a marked increase in the production of CH_2^+. An additional state at ~30 eV has been observed by several investigators[19,20] and has been ascribed to CH_4^+ in the configuration $(2a_1)^2$ $(1f_2)^4$ $(3a_1)$ by Appell[27] although it has recently been suggested that the doubly charged methane ion appears at this potential.[28] In either case, this band corresponds to the removal of two bonding electrons from the $(1f_2)$ orbital and the resulting state should be strongly dissociative. The abrupt increase in the production of H^+ which occurs in this energy region is consistent with this interpretation. The rate of CH^+ production increases gradually in this region and levels off around 40 eV.

The distribution of energy among the fragmentation products in general, and CH^+ in particular, will depend upon the details of the dissociating state of CH_4^+. While this study has not selected particular dissociating states by using controlled ionization energy, etc., we may infer from the photoelectron spectra and the fragment branching ratios that a major fraction of CH^+ is produced following excitation of the CH_4^+ $(2a_1)^{-1}$ level. The doubly excited state at 30 eV might also be considered as a source of CH^+, however, this is not likely since the branching ratio of CH^+ shows no significant change at this energy.

The thermodynamic threshold for the production of CH^+ through the reaction

$$CH_4 + e^- \rightarrow CH^+ + H_2 + H + 2e^- \quad (4)$$

is 19.3 eV.[24] This value is a full 3 eV below the observed appearance potential for CH^+, offering the possibility for considerable internal excitation of the products, consistent with the observations made in the present study. At approximately 4.5 eV above the threshold for the process indicated in eq 4, a new process,

$$CH_4 + e^- \rightarrow CH^+ + 3H + 2e^- \quad (5)$$

becomes energetically allowed. Since a significant amount of CH^+ is produced following ionization of methane by electrons with energies of 23.8 eV or greater, it would seem that both processes 4 and 5 can contribute to its formation. The large amount of rotational excitation in the CH^+ fragment, however, requires that the loss of 3H in eq. 5 occur non-symmetrically. On the basis of simple kinetic arguments the first step in the dissociation process leading to the production of CH^+ is probably hydrogen atom elimination. The loss of H_2 as a first step should be much less likely since this process may be considered a three center elimination as opposed to the two center hydrogen atom elimination.

In any unimolecular dissociation resulting in two products (CH^+ and H_2 in this case) the maximum kinetic energy of the two fragments may be calculated from simple classical mechanics. Any internal excitation (vibrational or electronic) will result in a reduced kinetic energy however, the exact partitioning of

internal excitation will depend upon the details of the potential energy surfaces involved. If one assumes that the dissociation exothermicity of CH^+ production from CH_4 is essentially the same as that of CD^+ production from CD_4 then the similarity in the rotational temperatures of CH^+ and CD^+ is easily understood. A simple analysis shows that the maximum kinetic energy of the CH^+ and CD^+ produced from CH_3^+ and CD_3^+ respectively are nearly the same with the CD^+ kinetic energy being slightly larger. While the fragment kinetic energies have not been measured in this study the rotational population distributions resulting from the dissociation "kick" have been studied and the same qualitative trends observed. While the vibrational population distribution could be modeled using approximations such as the impulse approximation for the collisional excitation of a classical anharmonic oscillator[29] the unusual distribution actually observed suggests the importance of more detailed potential surface factors.

The absence of product CH^+ below 22.3 eV simply reflects the inability of CH_4 to absorb energy between 17 eV and 22.3 eV. The efficiency of energy absorption is reflected in the intensity profiles seen in the photoelectron spectra (Fig. 19a). When CH_4^+ is formed in the $(2a_1)^{-1}$ state it must be assumed to be highly vibrationally excited due to the large change in equilibrium bond length. The subsequent decomposition of these vibrationally excited levels is seen in the sudden increase in CH_2^+ production as well as the onset of CH^+ production.

Since there are several eV released in the formation of CH^+ it is energetically possible to produce CH^+ in the $A^1\Pi$ state (T_e = 2.98 eV). It is clear from the analysis of the

internal energy distributions of CH^+ that some of this excess energy is channeled into vibrational and rotational excitation of the fragment. The CH^+ produced in the $A^1\Pi$ state radiates quickly[3] ($\tau \simeq 800$ nsec) down to the $X^1\Sigma^+$ state. Such radiative relaxation very nearly preserves the rotational distribution since $\Delta J = 0, \pm 1$ for such a transition. The vibrational distribution of CH^+ $X^1\Sigma^+$ produced through radiative relaxation of the A state will be largely determined by Franck-Condon factors, resulting in a relationship between vibronic populations which will, in general, be non-Boltzmann. Since the product distribution of electronic states was not determined in the present investigation, the initial vibrational distributions of either electronic state cannot be determined from the observed band intensities. It is interesting, however, to note that the rotational distributions of $v'' = 0$ and $v'' = 1$ for both CH^+ and CD^+ can be characterized by a single temperature to within the accuracy of our intensity measurements. This would imply that either the CH^+ (CD^+) is formed predominantly in a single electronic state, or that the product rotational distribution is very nearly independent of the vibrational/electronic energy distribution.

ACKNOWLEDGMENT

This work was supported by the Director, Office of Energy Research, Office of Basic Energy Sciences, Chemical Sciences Division of the U. S. Department of Energy under Contract Number W-7405-ENG-48.

REFERENCES

1. R. J. Cody, M. J. Sapety-Dzvonik and W. M. Jackson, J. Chem. Phys. 66, 2145 (1977).
2. C. M. Millar and R. N. Zare, Chem. Phys. Lett. 71, 376 (1980).
3. B. H. Mahan and A. O'Keefe, Ap. J. (in press).
4. F. J. Grieman, B. H. Mahan, and A. O'Keefe, J. Chem. Phys. 72, 4246 (1980).
5. F. J. Grieman, B. H. Mahan, A. O'Keefe, and J. Winn, Disc. Faraday Soc. 71, 16 (1981).
6. F. J. Grieman, B. H. Mahan and A. O'Keefe, J. Chem. Phys. 74, 857 (1981).
7. B. H. Mahan and A. O'Keefe, J. Chem. Phys. 74, (1981).
8. R. D. Knight and M. H. Prior, J. Appl. Phys. 50, 3044 (1979).
9. A. E. Douglas and J. R. Morton, Ap. J. 131, 1 (1960).
10. A. Antić-Jovanović, V. Bojović, D. S. Pesić, and S. Weniger, J. Mol. Spec. 75, 197 (1979).
11. Molecular Spectra and Molecular Structure, I, G. Herzberg, D. Van Nostrand Co. Inc., Third Printing 1953.
12. Prof. A. Carrington and co-workers have recently communicated to us their recent observation in emission of several new vibronic bands of CH^+, however, their final analysis has not yet been published.
13. S. Green, S. Hornstein and C. F. Bender, Ap. J. 179, 671 (1973).
14. K. E. Banyard and G. K. Taylor, J. Phys. B 8, L137, (1975).
15. P. Rosmus and W. Meyer, J. Chem. Phys. 66, 13 (1977).

16. I. Kusunoki and Ch. Ottinger, J. Chem. Phys. 71, 4227 (1979).

17. M. Carre, Physica, 41, 63 (1969).

18. M. Gérard, T. R. Govers and R. Marx, Chem. Phys. 30, 75 (1978).

19. C. Backx, G. R. Wright, R. R. Tol, and M. J. Van der Wiel, J. Phys. B, 8, 3007 (1975).

20. M. J. Van der Wiel, W. Stoll, A. Hamnett and C. E. Brion, Chem. Phys. Lett. 37, 240 (1976).

21. D. Morrison and J. C. Traeger, Int. J. Mass Spec. and Ion Phys., 11, 289 (1972).

22. C. Backx and M. J. Van der Wiel, J. Phys. B. 8, 3020 (1975).

23. P. L. Kronebusch and J. Berkowitz, Int. J. Mass Spec. and Ion Phys. 22, 283 (1976).

24. D. Mathur, J. Phys. B. 13, 4703 (1980).

25. C. A. Carlson and H. L. Strauss, Proc. Roy. Soc. (London) A, 269, 443 (1962).

26. W. Meyer, J. Chem. Phys. 58, 1017 (1973).

27. J. Appell, Thesis, Université Paris-Sud (1972).

28. T. Ast, C. J. Porter, C. J. Proctor and J. H. Beynon, Chem. Phys. Lett. 78, 439 (1981).

29. B. H. Mahan, J. Chem. Phys. 52, 5221 (1970).

Figure Captions

Fig. 1. Schematic representation of the experimental arrangement used in the present study. The phototube used to monitor laser induced fluorescence is positioned on top of the ion trap and views the fluorescence through the wire mesh on the top electrode. Obvious essentials, such as the encasing vacuum chamber, have been omitted from the figure.

Fig. 2. Portion of the laser induced fluorescence spectrum obtained for CH^+. Components of the $A^1\Pi$ - $X^1\Sigma^+$ (0,0) and (2,1) bands can be discerned in the spectrum which is normalized for variations in laser power.

Fig. 3. Portion of the laser induced fluorescence spectrum obtained for CD^+. As in Fig. 2 members of the (0,0) and (2,1) bands can be seen.

Fig. 4. Transitions observed near the (1,2) bandhead of the CD^+ $A^1\Pi$ - $X^1\Sigma^+$ system. While the signal to noise ratio is poor compared to that seen for the other bands it permits the calculation of the ground state vibrational frequency.

Fig. 5. Plot showing the determination of the rotational temperature for v=0 of the $X^1\Sigma^+$ state of CH^+.

Fig. 6. Rotational temperature determinations for the v=0,1 levels of the $X^1\Sigma^+$ state of CD^+. The rotational energy distribution is the same in each level to within the accuracy of this determination.

Fig. 7a. Summary of available photoelectron spectra for CH_4 showing the energies and relative intensities of several bands. These bands correspond to the production of CH_4^+ in several electronic states. The data summarized here is taken from Refs. 19 and 20.

7b. Branching ratios for the various ions formed in the ionization of CH_4 as a function of ionization energy. Data is taken from Refs. 21-24.

This report was done with support from the Department of Energy. Any conclusions or opinions expressed in this report represent solely those of the author(s) and not necessarily those of The Regents of the University of California, the Lawrence Berkeley Laboratory or the Department of Energy.

Reference to a company or product name does not imply approval or recommendation of the product by the University of California or the U.S. Department of Energy to the exclusion of others that may be suitable.

TECHNICAL INFORMATION DEPARTMENT
LAWRENCE BERKELEY LABORATORY
UNIVERSITY OF CALIFORNIA
BERKELEY, CALIFORNIA 94720